Neural Mechanisms of Sequential Dependence in Time Perception: The Impact of Prior Task and Memory Processing

Si Cheng (程思)[1], Siyi Chen (陈思佚)[1], Stefan Glasauer[2], Daniel Keeser[3], Zhuanghua Shi (施壮华)[1,3]

[1] General and Experimental Psychology, Department of Psychology, LMU Munich, Munich, Germany

[2] Computational Neuroscience, Brandenburg University of Technology Cottbus-Senftenberg, Cottbus, Germany

[3] NeuroImaging Core Unit Munich (NICUM), LMU Munich, Munich, Germany

Author note

This study was supported by German research foundation (DFG) research grants SH 166/ 3-2 to Z.S GL 342/3-2 to S.G. and CH 3093/1-1. The NICUM scanner was financed by the DFG project 324324095. Correspondence concerning this article should be addressed to Si Cheng, email: chengsi123456@gmail.com, General and Experimental Psychology, Department of Psychology, LMU Munich, 80802 Munich, Germany.

Abstract

Our perception and decision-making are susceptible to prior context, as seen in sequential dependence where our judgment of stimulus magnitude is biased toward what we experienced in previous trials. While sequential bias in the spatial domain has been extensively studied, less is known about it for time perception. Furthermore, it is still debatable whether sequential bias arises during perceptual or post-perceptual stages. To investigate this, we conducted functional magnetic resonance imaging (fMRI) on twenty-one participants performing a timing task, which involved two phases - duration encoding and duration reproduction. Participants had to remember the duration of the green coherent motion and wait for a cue to reproduce the perceived duration. The cue could be either "Go" or "No-go". For the "No-go" cue, participants should only passively view the display. We observed that the reproduction error was positively correlated with the prior duration only when the preceding task was also active reproduction. In contrast, encoding the prior duration without reproduction was insufficient to induce sequential bias. Neurally, we observed activated timing-related networks, such as striato-thalamo-cortical circuits, and performance monitoring networks when the trial sequence implicitly predicted a "Go" trial. When action required a post cue, the right frontal gyrus, associated with response inhibition, became activated. Importantly, the hippocampus showed sensitivity to sequential bias and its activation was negatively correlated with the individual's sequential bias following active reproduction trials. These findings highlight the crucial role of striato-thalamo-cortical networks in time perception, as well as memory networks in sequential biases at the post-perceptual stage.

Keywords: Sequential dependence; Time perception; fMRI; striato-thalamo-cortical networks; Hippocampus; Working memory

Significance Statement

This study explores the neural mechanisms measured by fMRI underlying time perception and the factors that can influence our time judgments across trials. Our findings reveal that active estimation of time duration in the previous trial can bias subsequent estimates, resulting in a sequential bias. In contrast, passive viewing of a stimulus without reproducing its duration does not produce this effect. At the neural level, we observed increased activity in memory regions like the hippocampus when sequential biases were reduced. Furthermore, we found a negative correlation between hippocampal activation and sequential bias when the hippocampus was less active. Our findings suggest that the involvement of memory networks mediates how we are influenced by past experiences when judging time.

Introduction

Time perception is susceptible to various factors, including attention, memory, and temporal context (Wittmann, 2009; Shi et al., 2013a). For instance, the subjective duration can be biased toward recent history (Jazayeri and Shadlen, 2010; Shi et al., 2013a) or preceding durations (Nakajima et al., 1992; Burr et al., 2009; Glasauer and Shi, 2022), leading to an underestimation of long durations and overestimation of short durations. Such history contextual modulation has been long studied in terms of sequential dependence (Holland and Lockhead, 1968; Treisman and Williams, 1984), which refers to the influence of previous stimuli on the behavior of the current trial. The effect has been studied in the context of non-temporal features, such as orientation, color, and motion direction, particularly with a recent paradigm highlighting influences of the difference between the current and previous stimuli on response biases, referred to as serial dependence (Fischer and Whitney, 2014; Cicchini et al., 2017; Bae and Luck, 2020; Barbosa and Compte, 2020).

Serial dependence in vision is thought to maintain perceptual stability and continuity by integrating past and current information to filter out abrupt noises, serving as a perceptual mechanism (Liberman et al., 2016; Whitney et al., 2022). However, recent research has shown that task and response-related post-perceptual factors can also affect serial dependence (Fritsche et al., 2017; Pascucci et al., 2019; Bae and Luck, 2020; Ceylan et al., 2021). For instance, serial dependence is only observed when the current and previous tasks are the same orientation judgments (Bae and Luck, 2020). A recent fMRI study showed that neural activity in low-level V1 is opposite to behavioral serial dependence, which suggests that the effect emerges in high-level memory or decision-making circuits (Sheehan and Serences, 2022). Working memory also plays a crucial role in serial dependence, as it involves integrating preceding stimuli with current sensory inputs for decision-making and motor plans (Bliss et al., 2017; Kiyonaga et al., 2017; Bae and Luck, 2019; Fornaciai and Park, 2020a). Studies have shown serial dependence increases when the memory retention interval increases (Bliss et al., 2017), and decreases when the short-term memory maintenance in the premotor cortex is interrupted with TMS (de Azevedo Neto and Bartels, 2021).

The current body of research on serial dependence has primarily focused on non-temporal spatial features with a circular scale distribution (e.g., orientation). However, there has been limited investigation into serial dependence in time perception, with only a few studies examining trial-by-trial updating of internal models or priors (e.g., Dyjas et al., 2012; Glasauer and Shi, 2022), and no neural signature has been linked to it. In this study, we aimed to explore the neural mechanisms underlying sequential dependence in time perception using a duration reproduction task with MRI scanning. During the task, participants had to remember the duration of a stimulus, and either reproduce it or passively watch it, based on a post-cue. As time intervals are an open scale, we focused on how the previous stimuli bias current judgments (i.e., sequential dependence). To distinguish sequential dependence from the central tendency bias (Jazayeri and Shadlen, 2010; Shi et al., 2013a), we estimated relative errors by measuring the deviation from the mean reproduction for each individual duration and correlated it with the preceding duration. Our results demonstrate that sequential dependence was significant only when the preceding task involved active reproduction, not passive viewing. Using the general linear model (GLM) with fMRI data, we found that striato-thalamo-cortical timing and memory networks, including the hippocampus, were activated during the encoding of durations following passive viewing trials, which led to a reduction of sequential bias. We then further investigated the relationship between hippocampus BOLD activities and the sequential dependence effect, revealing a negative correlation between them across participants for trials with preceding active reproduction. These findings highlight the involvement of post-perceptual stages that link sensory representations and responses underlying sequential dependence in time perception and underscore the critical role of active timing and memory networks in protecting against sequential biases, indicating the involvement of short-term memory traces from the previous trial on sequential biases.

Materials and Methods

Participants

21 participants (9 females; 12 males; age: *Mean* ± *SD* = 27.24 ± 3.83, range: 23–33 years) were recruited for the two-session MRI experiment[1]. All of them were right-handed and had normal or corrected-to-normal vision and color vision, no history of neurological, psychiatric, or medical disorders, and no symptoms of COVID-19 in the past two weeks. The sample size was determined based on previous studies (Fischer and Whitney, 2014; Bae and Luck, 2020) that usually found large effect sizes (Cohen's d > 0.753), and with a power of 80% ($1 - \beta$), which yielded a minimum of 19 participants according to G*Power (Erdfelder et al., 1996). Participants provided their informed consent prior to the experiment and were compensated for their participation for 15 Euro/hour. The study was approved by the ethics committees of the Psychology Department at LMU Munich.

Experimental design and procedure

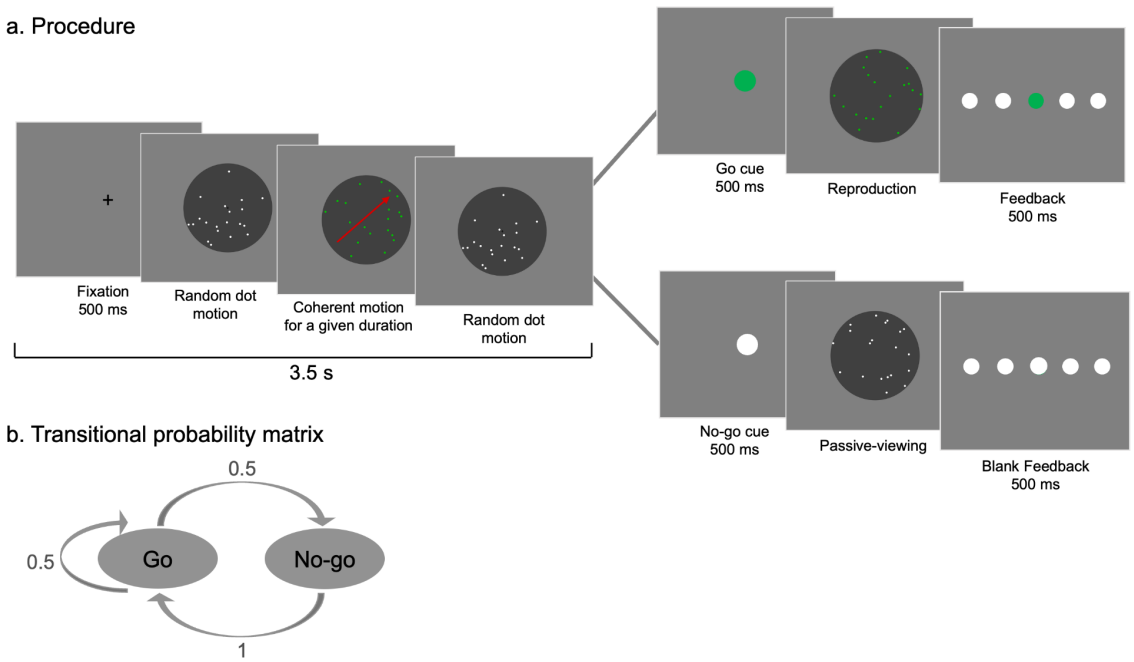

Figure 1 (**a**) Schematic illustration of the experimental procedure. The experiment consisted of two phases: the duration encoding phase and the duration reproduction or passive-viewing phase, with the

[1] During scanning, six participants had large head movements (more than 3 mm of displacement measured by 2nd degree B-spline interpolation or 3° of rotation in any direction) or distortion in the T1 image. We then replaced with six new participants.

latter being contingent upon the Go / No-go cue. The trial started with a fixation, followed by the display of white random dot motion, which then changed to green dots moving coherently in one direction (e.g., in the direction of the red arrow in the illustration, not shown in the actual experiment) for a given duration before reverting back to white random dot motion. The entire presentation of the dots display lasted for 3000 ms. Participants were instructed to remember the duration of the green coherent motion. A cue, either a green ("Go" trial) or white ("No-go" trial) disk, was then shown on the screen, indicating the beginning of the second phase. In the "Go" trials, the green random dot motion appeared, and participants had to press a button when they thought the duration was the same as the perceived duration in the encoding phase. During "No-go" trials, participants only passively viewed the white random dot motion for the same duration as the coherent movement of the green dots in the encoding phase and were not required to respond. In the end, there was a feedback display featuring five horizontal white disks, with one disk changing color to indicate the accuracy of the reproduction for the "Go" trials. (**b**) The inter-trial transitional probability between the Go and No-go trials. This transitional structure guarantees equal probability of "Go to Go" and "No-go to Go" trials.

We adopted a duration reproduction paradigm (Shi et al., 2013b, 2022; Zang et al., 2022), consisting of an encoding phase and a reproduction phase (see Figure 1). Participants laid down comfortably with their head in the head coil, inside some cushions to fixate the head position and avoid motion. Participants viewed the back projector canvas (diagonal 30 inches) via an adjustable mirror positioned on top of the head coil, with a viewing distance of 110 cm. The task was presented by an MRI-compatible ProPIXX DLP LED projector (Pixx Technologies Inc, Canada).

Each trial began with a black cross (visual angle of 0.5°) at the center of the display on a light gray background for 500 ms, prompting participants to maintain their fixation on the center. Following this, a tunnel view display (subtended 17.8° visual angle) of white randomly moving dots (20 dots with each diameter of 0.4°, moving at a speed of 1 °/s) appeared for a randomly selected duration between 400 to 600 ms. The white dots then changed to green and moved 100% coherently with a speed of 6°/s in one direction selected between 0 to 360° for a given duration, chosen from 0.8, 1.0, 1.2, 1.4, and 1.6 secs. Immediately after the given duration, the color of the dots changed back to

white and moved randomly again at a speed of 1 °/s. When a dot exited the tunnel view, it was regenerated at a random location within the view to maintain dot density. The entire presentation of the tunnel view lasted for 3000 ms. Participants were instructed to remember the duration of the green coherent motion.

Following the encoding phase, a cue was presented in the center for 500 ms that indicates whether participants should perform a reproduction task ("Go") or not ("No-go"). The cue was a color disk (subtended 1.2° visual angle), which could be either green (indicating a Go trial: reproducing the duration) or white (indicating a No-go trial: doing nothing, only passive viewing). For Go trials, immediately following the offset of the cue display, a green random dot motion in a tunnel view (20 green dots with each of 0.4° at a speed of 1°/s) appeared in the center of the screen. Participants had to monitor the elapsed time and press an MRI-compatible ResponsePixx button (Pixx Technologies Inc, Canada) with their right thumb when they perceived the elapsed time as being the same as the duration of coherent movement in the encoding phase. Following the response, a feedback display appeared indicating the response accuracy with a color dot in a horizontal dot array. Each highlighted dot from the left to right five dots corresponded to a range of relative reproduction errors (error / duration): The left most represented below -30%, while the second to fifth dot indicated errors between [-30%, -5%], (-5%, 5%), [5%, 30%], or greater than 30%, respectively. The middle dot was highlighted in green to indicate an accurate reproduction, while the 2nd and 4th dots were highlighted in light red, the utmost 1st and 5th dots in dark red, with the color intensity reflecting the degree of error. The feedback lasted for 500 ms. For the No-go trial, the cue display was followed by a white random dot motion in a tunnel view (20 white dots with each diameter of 0.4°, moving at a speed of 1°/s), lasting the same amount of time as the coherent movement of the green dots in the encoding phase, and participants didn't need to respond and just passively watched the display. Afterward, a blank feedback display appeared for 500 ms to equate the time with the feedback display in the Go trial. The next trial started after a random interval of 2000 to 3000 ms.

Since we were interested in the impact of the preceding task on the present reproduction, and to ensure equal transitional probability from a No-go to Go trial and from a Go to Go trial while minimizing the number of trials required for MRI scanning (within one hour), we excluded the

possibility of a No-go to No-go trial (see Figure 1b). This yielded a 2:1 ratio of the Go vs. No-go trials while maintaining equal transitional probability (see a similar approach Czoschke et al., 2019).

Prior to the formal scanning, participants received a practice block of 30 trials to familiarize themselves with the task in a sound-reduced and moderately lit chamber, near the scanning room. In the formal MRI study, each participant completed 12 blocks, with each block of 30 trials, among them 20 Go trials and 10 No-go trials. After each block, there was a short 6-second break, and after 6 blocks (comprising a session) a long 7-minute break. During this long break, participants took a rest inside the scanner, and a T1 image was acquired. The whole experiment lasted approximately 60 minutes.

MRI data acquisition and preprocessing

All MRI data were acquired using a 3-Tesla Siemens Prisma MRI scanner (Siemens, Erlangen, Germany), equipped with a 32-channel head coil. Functional MRI images were obtained using a blood oxygenation level-dependent (BOLD) contrast-sensitive gradient-echo EPI sequence. A total of 3000 to 3300 volumes of fMRI data, depending on the duration of the experiment, were acquired for each participant through two sessions. The following parameters were used: TR = 1000 ms, multi-band factor = 4, TE = 30 ms, flip angle = 45◦, FOV = 210 × 210 mm, voxels size = 3 × 3 × 3 mm, slices number = 48, slice thickness = 3 mm. In addition, structural MRI images (T1 weighted) were acquired from the sagittal plane using a three dimensional magnetization prepared rapid gradient-echo (MPRAGE) pulse sequence with the following scanning parameters: TR = 2500 ms, TE = 2.22 ms, flip angle = 8◦, FOV = 256 × 256 mm, voxel size = 0.8 × 0.8 × 0.8 mm, slice thickness = 0.8 mm.

The analyses and visualization of imaging data were performed with SPM12 (Ashburner et al., 2014) and Nilearn - 0.9.2 (Abraham et al., 2014). The functional images were first preprocessed with realignment, reslicing, and slice time correction. Then, the head movement correction was done by using affine transformation in a two-pass procedure and aligning individual functional images to their mean image using 2nd degree B-spline interpolation. Participants who had head movements more than 3 mm or rotations greater than 3° were excluded from further analysis, which yielded the

exclusion of six participants in total, five for large head motion and one for T1 image distortion. We then replaced it with six new participants. The mean image of each participant was then spatially normalized to a 3mm standard Montreal Neurological Institute (MNI) template using the "unified segmentation" approach, and the resulting deformation field was applied to the individual functional images. The normalized fMRI images were then smoothed with a 6 mm full-width-at-half-maximum (FWHM) Gaussian kernel to improve the signal-to-noise ratio and compensate for residual anatomical variations.

Statistical analyses

Behavioral analysis

The reproduction biases, the difference between the reproduced duration and the physical duration, were calculated for the Go trials. Overall, reproduced durations were close to the probe durations, resulting in a mean reproduction bias of 35 ms. To exclude trials with large reproduction errors due to accidental button presses or inattention, we applied the three-sigma rule to exclude those outliers. The outliers were generally rare, on average only 0.89%, ranging individually from 0 to 5 outlier trials. Then, we categorized the remaining Go trials into two types depending on the preceding task: (a) Go-Go (GG) trials that were preceded by a reproduction task, and (b) Nogo-Go (NG) trials that were preceded by a passive viewing task.

Given that duration reproduction (D_r) is affected by both the central tendency effect and the short-term sequential dependence (Glasauer and Shi, 2022), we estimated the central tendency and serial dependence effects separately. The central tendency effect results from the integration of the prior (D_p) and the current duration (D_n), which can be approximated using linear regression when the prior is assumed to be unchanged (Cicchini et al., 2012; Shi et al., 2013a):

$$D_r = wD_n + (1 - w)D_p .$$

Thus, here we applied a linear regression to obtain the slope (w), and used $1 - w$ as the central tendency index, with 0 indicating no central tendency and 1 strong central tendency.

To assess the sequential dependence of time perception, we first eliminated the general bias by subtracting the mean reproduction for each sample duration from the trial-level reproduced duration, then normalized the error in a relative term for each subject:

$$RE_{i,k} = (D_{i,k} - \bar{D}_k)/\bar{D}_k ,$$

where $\bar{D}_k$ is the mean reproduction at duration D_k, $D_{i,k}$ the reproduced duration at trial i of a given Duration D_k, $RE_{i,k}$ the normalized relative error. Second, given the duration is an open-scale measure, we applied a linear regression with the normalized relative error to the previous sample duration (D_{n-1}), and took the slope of the linear fit as the sequential bias index (Cicchini et al., 2014, 2018; e.g., Glasauer and Shi, 2022). A positive slope indicates that the current estimation is attracted towards the previous duration (henceforth referred to as the "sequential dependence effect"), while a negative slope indicates that the current time estimation is repulsed from the previous duration.

For statistical analyses, we applied linear mixed model analysis, repeated measures ANOVA, and simple t-tests according to the data structure. Linear mixed models are robust to sphericity violations and do not inflate Type I errors (Singmann and Kellen, 2019) and they can accommodate the covariant factor (duration) in addition to the fixed effects addressed by ANOVA. The *p*-values reported for the mixed models were calculated using the maximum likelihood estimation.

fMRI statistical analysis

There were three types of inter-trial transitions: No-go to Go (NG), Go to Go (GG), and Go to No-go (GN). Given that the third type (GN) trials yielded no behavioral response, the main analysis was focused here on the Go trials (i.e., GG and NG). To ensure a comprehensive view of brain activities, we also reported analysis with the GN trials in the Appendix. To boost the power of the first-level fMRI analyses, we grouped the preceding durations into two categories: the "Short" and the "Long" categories. The "Short" category included durations of 0.8 and 1.0 s, and the "Long" categories were 1.4 and 1.6 s, with the middle duration of 1.2 s being excluded. Once the regions of interest (ROIs) were identified, we proceeded with a comprehensive analysis where all durations were taken into account.

At the first-level analysis with individual participants, BOLD responses obtained from the smoothed images were time-locked to the onset of the target duration and modeled using a canonical hemodynamic response function (HRF) with a box-car function to represent the duration of the coherent movement. A combination of the factor of the Prior Task (GG or NG) and the categorical Prior Duration (Short or Long) resulted in four conditions, each represented by a separate main HRF regressor. To reflect the true modulation of sequential bias, we used the normalized relative error $RE_{i,k}$ as an additional parametric regressor for each of the four main regressors, similar to previous studies (Penny et al., 2011; Mumford, 2015), four parametric modulators in total. Additionally, six head movement parameters were added as nuisance regressors to control head motion artifacts (Lund et al., 2005). The data were high-pass filtered at 1/128 Hz. For each subject, 8 condition-specific contrast images were created (for each trial type and parametric modulator).

The respective contrast images for the main HRF regressors and the parametric regressors were subjected to the second-level analysis with flexible factorial design, separately. In the flexible factorial design, Prior Task and Prior Duration were created as within-subject factors and Participant as a random factor. The 2 (Prior Task: Go vs. No-Go) × 2 (Prior Duration: Short vs. Long) ANOVAs allowed us to determine the unique contributions of each factor to brain activity, and how they might interact with each other to affect neural processing. We conducted a whole-brain analysis to determine the candidate brain regions involved in the main effects of Prior Task and Prior Duration, as well as their interaction, by using planned t-contrasts. All contrasts were thresholded at $p < .001$, with FWE cluster correction at $p < .05$. We focused on brain regions that showed sensitivity to the modulation of brain activity by the normalized relative deviation. Parameter estimates were extracted from the statistically significant clusters and averaged across the voxels in the individual-level analyses.

To gain further insight into activation patterns, a separate general linear model (GLM) was applied to the fMRI time series, similar to the model designed above, except all individual durations were included (0.8, 1.0, 1.2, 1.4, and 1.6 s). Thus, we have 2 (Prior Tasks) × 5 (Prior Durations), 10 conditions in total. Each condition had one main HRF regressor and one parametric regressor using the normalized relative error. β values of individual main regressor as well as parametric modulator

were calculated from the significant voxels detected above (a sphere with a diameter of 10 mm) for individual participants. To assess the changes in the BOLD signal and the parametric modulation in the brain activity, a linear mixed model analysis with Prior Task and Prior Duration as the fixed effects and Subject as the random factor was applied to the β values of the main regressor as well as the parametric modulator.

We then conducted Spearman's correlation (α = 0.05, two-tailed) to assess the relationship between the magnitude of the serial dependence effect in behavior and the BOLD activity of interest. The slope of the linear regression with the normalized relative error depending on the previous sample duration was operationalized to indicate the magnitude of the behavioral serial dependence effect. The BOLD response was measured as the β values of the main regressors in the designated regions detected above.

Results

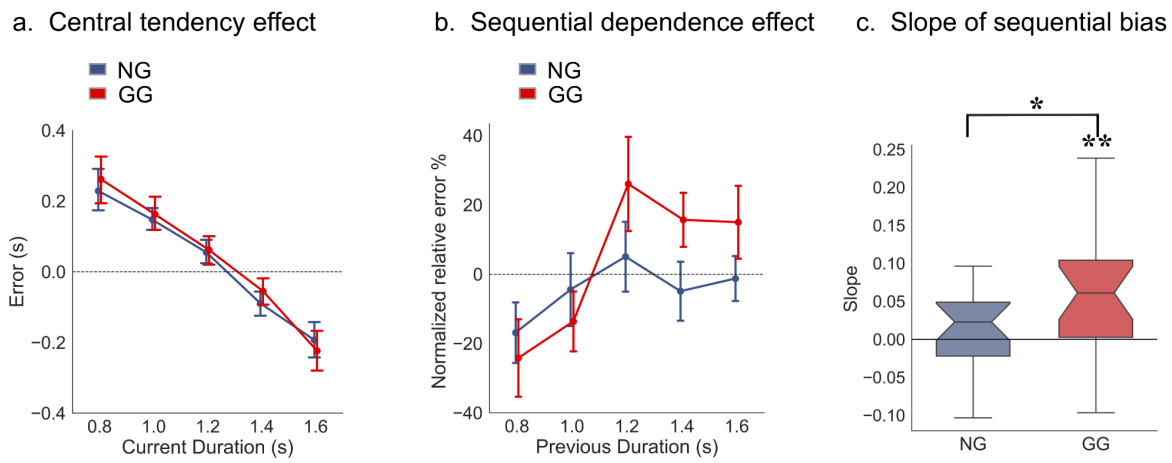

Figure 2 (**a**) The central tendency effect. The reproduction errors (i.e., reproduced duration - actual duration) are shown as a function of the actual duration, separated for the inter-trial type: Go/Go (GG) and No-go/Go (NG) trials. (**b**) The sequential dependence effect. The normalized relative errors are plotted on the durations from previous trials, separated for NG and GG conditions. Error bars represent the standard error of the mean. (**c**) Notched boxplots of the sequential dependence slope for

NG and GG conditions. The box plot depicts the serial dependence effect, measured by the slope, for each condition. The top and bottom of the notched box represent the interquartile range (between 25% and 75%), and the notch in the box is the 95% confidence interval for the median; whiskers exclude outliers. *p <.05,**p <.01.

Behavioral results

The central tendency effect.

The results, shown in Figure 2a, indicate a strong central tendency effect - participants overestimated short durations and underestimated long durations. The central tendency effect was quantified through linear regression, revealing significant central tendency biases with mean slopes of -0.540 ($t_{(20)}$ = -9.14, p <.001, d = 1.99) and -0.594 ($t_{(20)}$ = -9.13, p <.001, d = 1.99) for the NG and GG respectively. But the central tendency biases were comparable between the two conditions ($t_{(20)}$ = 1.745, p = .096, BF_{10} = 0.826). Additionally, there was a minor positive general bias ($M \pm SE$: 35 ± 14 ms, $t_{(20)}$ = 2.45, p = .024, BF_{10} = 2.49), which was comparable between the two conditions ($t_{(20)}$ = -1.3, p = .21, BF_{10} = 0.48). That is, the central tendency and the general bias were not influenced by the prior trial task. The lack of a significant difference in the central tendency effect between preceding task types might be primarily due to the same distribution and range of the tested durations for two prior tasks, yielding a consistent long-term representation of the prior durations across tasks. This agrees with previous findings that randomly mixing durations leads to a generalization of the prior across conditions (Roach et al., 2017).

The sequential dependence effect.

The normalized relative error $RE_{i,k}$ was used to analyze the sequential dependence. Our results, presented in Figure 2b, show that the normalized relative error increases with the preceding duration, suggesting the sequential bias can be approximated by a linear relation. Thus, to characterize the sequential dependence effect, we employed a linear mixed model with Prior Task and Prior Duration as the fixed effects and Subject as the random factor. Our analysis revealed that the normalized relative error was significantly correlated with the preceding duration (slope b = 0.055,

95% *CI* = [0.024, 0.085], $p < .001$) for the GG condition. That is, the sequential bias increased 5.5% with each one-second increase in the preceding duration. However, the linear trend for the NG condition failed to reach significance (slope b = 0.016, 95% *CI* = [-0.014, 0.047], $p = .298$). The main effect of the Prior Task was not significant ($b = 0.008$, 95% *CI* = [-0.02, 0.004], $p = .191$), as relative errors were symmetric around the mean of the preceding duration for both NG and GG conditions (Figure 2b). To determine whether the active reproduction, relative to the passive viewing, in the preceding trial increased the sequential dependence on the current reproduction, we compared the slopes of the GG condition to the NG condition, which revealed the slope was significantly larger in the GG condition ($t_{(20)} = 2.229$, $p = .037$, $BF_{10} = 1.716$). These results suggest that active reproduction in the preceding trial increased the sequential dependence on the current reproduction, whereas passive viewing did not.

To avoid statistical artifacts (Cicchini et al., 2014), we also tested the sequential dependence effect on the durations presented in future trials (n+1), which showed no significance (*ps* > .216). Our behavioral results provide clear evidence that merely passively perceiving an interval is not sufficient to bias subsequent duration estimates.

fMRI Results

Whole-brain analysis

The imaging data were analyzed using a random-effects GLM following a 2 (Prior Task: Go vs. No-go) × 2 (Prior Duration: Short vs. Long) factorial design. Each condition was represented by a main HRF regressor and a parametric regressor. The results from the main regressors reflect different brain activations between conditions, while the findings of the parametric regressors reflect the covariate changes of brain activities to the normalized relative errors in duration reproduction. In the following subsections, we report the results separately for the main HRF regressors and parametric regressors.

Table 1. Activations associated with the main HRF regressors defined by the two factors Prior Task and Prior Duration

Contrast	Region label	MNI coordinates			Cluster size	T value
Prior Task						
GG > NG	R inferior frontal gyrus	45,	41,	2	109	5.42
NG > GG	R Posterior medial frontal	6,	-1,	53	8003	6.34
	R Thalamus	9,	-22,	5		6.09
	L Precentral gyrus	-30,	-16,	50		7.46
	L Postcentral gyrus	-51,	-19,	53		6.72
	L Precuneus	-9,	-61,	14	259	3.64
Prior Duration						
Long > Short	R Caudate Nucleus	18,	-22,	26	122	4.42
Prior Task* x *Prior Duration	n.s.					

Note: Activations were significant at $p < .001$, with FWE cluster correction at $p < .05$, and n.s. denotes non-significant. R Posterior medial frontal, R Thalamus, L Precentral gyrus, and L Postcentral gyrus were in the same cluster.

Table 2. Activations associated with the parametric regressors defined by the two factors Prior Task and Prior Duration

Contrast	Region label	MNI coordinates			Cluster size	T value
PriorTask	n.s.					
Prior Duration						
Long > Short	L Middle frontal gyrus	-21,	38,	32	124	4.46
Prior Task* x *Prior Duration						
Long (NG > GG)	L Hippocampus	-36	-37,	-7	139	4.09
	R Hippocampus	39,	-31,	-7	305	5.01

Notes: Activations were significant at $p < .001$, with FWE cluster correction at $p < .05$, and n.s. denotes non-significant.

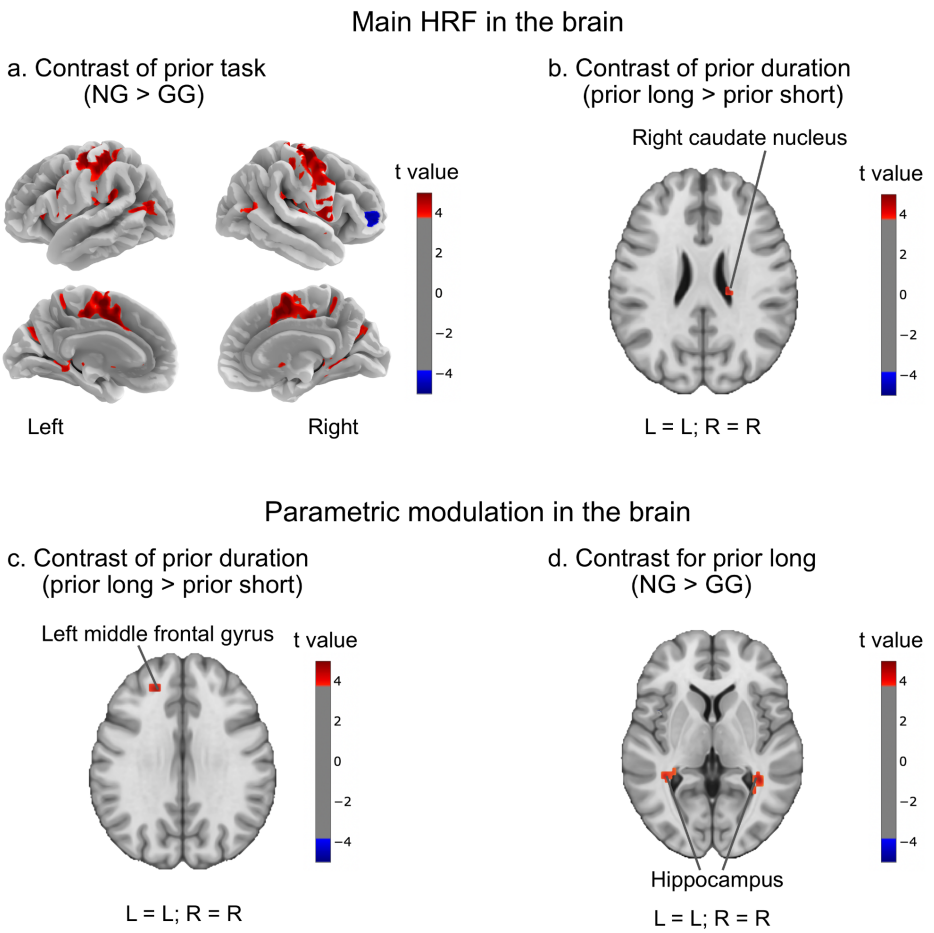

Figure 3. Whole-brain activation results. (**a**) and (**b**) are brain regions activated in the main HRF. (**a**) Whole-brain activation patterns colored in red-blue reflected invoked BOLD signals driven mainly by the prior task. The red-marked regions (the left precentral gyrus, the left postcentral gyrus, the left precuneus, and the right posterior-medial frontal, the right thalamus) were activated more for the preceding No-go (NG) task as compared to the preceding Go task (GG), while the blue-marked region (right inferior frontal gyrus) were activated more for the GG than the NG condition. (**b**) Whole-brain activation patterns colored in red-blue reflected invoked BOLD signals that were driven by the prior duration. The red-marked region (right caudate nucleus) was activated more for the long duration as compared to the short duration. (**c**) and (**d**) are brain regions that show sensitivity to normalized relative error in different conditions. (**c**) Main effect of prior duration for the parametric estimates with the normalized error. The red-marked region (left middle frontal gyrus, MNI coordinates: -21, 38, 32) was activated more with a larger normalized relative error for the preceding long duration than the short duration. (**d**) The normalized error-dependent differences between prior tasks (NG vs. GG)

in the prior long-duration condition were expressed in the hippocampus (MNI coordinates: -36, -37, -7; MNI coordinates: 39, -31, -7). All thresholding was done at $p < .05$ with FWE-corrected at the clustered level. Neurological convention was used (L = L and R = R).

Main HRF regressors

We conducted contrast analyses using 2 (GG vs. NG) × 2 (Short vs. Long) within-subject ANOVAs. Table 1 and Figure 3a and 3b show the significant regions identified through this contrast analysis. The results show that the right inferior frontal gyrus (RIFG), a region associated with response inhibition (Aron et al., 2007; Hampshire et al., 2010), exhibited greater activation during GG trials compared to NG trials. Conversely, the left precuneus and a large cluster comprising the left precentral gyrus and left postcentral gyrus and the right posterior-medial frontal and the right thalamus were more active during NG trials compared to GG trials.

The RIFG is a critical region for response inhibition and detecting important cues (Aron et al., 2007; Hampshire et al., 2010). The activation of the RIFG for the contrast GG vs. NG is likely due to an active present trial (G) having a 50% chance of requiring response inhibition (No-go, a G trial can be followed by G or N) while a passive trial (N) predicted 100% of active reproduction (NG, see Figure 1b). In contrast, for the contrast NG vs. GG, we observed high activation in cognitive control and performance monitoring networks, including the right posterior-medial frontal cortex (Debener et al., 2005) and the left precentral gyrus and left postcentral gyrus, as well as the left precuneus (Ridderinkhof et al., 2004; Fitzgerald et al., 2010). Increased activation in the posterior-medial frontal cortex (Ridderinkhof et al., 2004; Fitzgerald et al., 2010) is believed to be engaged in the cognitive control and performance monitoring that leads to response selection and performance adjustments on subsequent trials (Debener et al., 2005), while the precentral gyrus is the site of the primary motor cortex and the postcentral gyrus which constitutes the primary somatosensory cortex also takes part in motor control of the body (Hari et al., 1998; Chris Dijkerman and de Haan, 2007). This was likely due to the activation of the primary motor cortex for those 'Go' trials while not for the 'No-go' trials. Further analysis of 'No-go' (GN) trials revealed 'negative' activation in those motor-related areas (see Appendix). A simulation indicated that the activation patterns in the primary motor cortex with NG

trials could be explained by early motor activation compared to GG and GN trials. This is likely due to the sequential structure of NG, which already indicates that the upcoming reproduction is a "Go" trial before the cue appears (see the simulation in the Appendix).

The thalamus plays a key role in the cortico-thalamic-basal ganglia timing circuits (Mole et al., 2018; Yin et al., 2022). The contrast analysis conducted between the prior short and long durations revealed that the right caudate nucleus, the main component of the dorsal striatum, was more activated when the prior trial was long than short (see Table 1 and Figure 3b). The activity in the dorsal striatum (including the caudate nucleus) is closely related to the representation of temporal information in working memory (White, 2009; Merchant et al., 2013; Teki and Griffiths, 2016; Yin et al., 2022). In the current study, preceding long vs. short durations might impact the working memory trace in the following trial, consistent with previous event-related fMRI studies on working memory and time interval demonstrating that activity in the caudate nucleus increased with an increasing number of intervals in the sequence (Rao et al., 2001; Coull and Nobre, 2008; Teki and Griffiths, 2016).

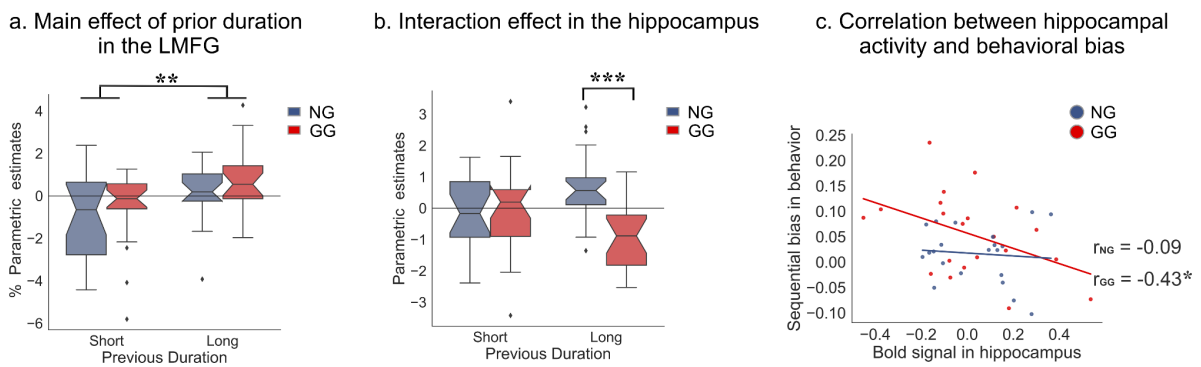

Figure 4 (**a**) Notched boxplots for the mean parameter estimates (β) from the left middle frontal gyrus (LMFG) for the parametric regressor for the prior tasks (NG: No-go; GG: Go), separated for the category of the previous duration (Short vs. Long). The top and bottom of the notched box represent the interquartile range (between 25% and 75%), and the notch in the box is the 95% confidence interval for the median; whiskers exclude outliers. (**b**) Notched boxplots for the mean parameter estimates (β) from the hippocampus for the parametric regressor. (**c**) Correlations between the mean BOLD signal in the bilateral hippocampus (MNI coordinates: -36, -37, -7, including 139 voxels; MNI

coordinates: 39, -31, -7, including 305 voxels) and the behavioral bias (slopes of the linear regression with the normalized errors to the previous sample duration) across participants, separated for the GG and NG conditions. The correlation was significantly negative for the GG condition (r_{GG}= -.43, p < .05), but not for the NG (r_{NG} = -.09). The least-square fit lines are shown. *p <.05, ***p< .001.

Parametric regressors

By using the normalized error, $(R_{i,k} - \bar{R}_k)/\bar{R}_k$, as a parametric regressor to exclude the central tendency and general biases, modulation of the parametric regressors would truly indicate how the sequential bias covaries with BOLD activation. The parametric value of the regressor reflects the strength and linear relationship between brain activity and the normalized error. Given that BOLD activations were analyzed during the encoding phase, while sequential biases were obtained during the late reproduction phase, a positive value indicates that increased brain activity leads to an increase in sequential bias, whereas a negative value suggests that increased brain activity results in a negative change in sequential bias. The contrast results can show which brain regions during the encoding stage are correlated with changes in sequential biases. Table 2 and Figure 3c and 3d show the contrasted results of the parametric regressors according to the 2 (Prior Task: Go vs. No-go) × 2 (Prior Duration: Short vs. Long) factorial analysis.

As seen in Table 2 and Figure 3c, the left middle frontal gyrus (LMFG; MNI coordinates: -21, 38, 32, including 124 voxels) was more positively correlated with the normalized error when the duration of the preceding trial was long vs. short. Figure 4a depicts the parametric values extracted from the left middle frontal gyrus. On average, the parametric value was positive (0.412) when the preceding duration was long, but negative (-0.691) when the preceding duration was short. This suggests that influences of the left middle frontal gyrus activation on normalized error depend on the preceding duration. Specifically, higher activation of the left middle frontal gyrus led to a positive relative error when the preceding duration was long, but a negative relative error when the preceding trial was short. Recall the right caudate nucleus was found to activate more strongly in response to a long preceding duration compared to a short one, and the right caudate nucleus is functionally

connected to the left middle frontal gyrus (Robinson et al., 2012), which is associated with working memory encoding (Nee et al., 2013; Dandolo and Schwabe, 2019). Given this association, it is possible that these two regions work together to regulate inter-trial dependence in duration judgments.

Additionally, the analysis revealed a significant Prior Duration × Prior Task interaction in the both left and right hippocampus (left MNI coordinates: -36, -40, -7, including 16 voxels; right MNI coordinates: 39, -31, -7, including 25 voxels; with small-volume correction at $p < .05$ FWE corrected). Further analyses revealed the most significant contrast results from the left and right hippocampus between GG and NG conditions when the preceding trial was long, which showed a difference between GG and NG was sensitive to the normalized bias (see Figure 3d, MNI coordinates: -36, -37, -7, including 139 voxels; MNI coordinates: 39, -31, -7, including 305 voxels). As shown in Figure 4b, on average the parametric values were comparable between NG and GG when the preceding duration was short, but exhibited opposite signs for the preceding long durations. In trials preceded by a long/No-go task, the more active the hippocampus, the higher the normalized errors. Conversely, in trials preceded by a long/Go task the less active the hippocampus, the higher the normalized errors.

We then further conducted a correlation analysis to examine the relationship between the sequential dependence effect (using the slope of sequential bias) and the BOLD signal in the hippocampus. The analysis revealed a negative correlation ($r = -.43$, $p = .049$, two-tailed; Figure 4c) for GG trials (for both short and long duration), suggesting more activation in the hippocampus leads to less sequential dependence for GG trials. However, there was no correlation for NG trials ($r = -.09$, $p = .69$, two-tailed; Figure 4c), partly because the activation in the hippocampus was generally higher for NG than GG trials (Figure 5a).

ROI analysis on the hippocampus

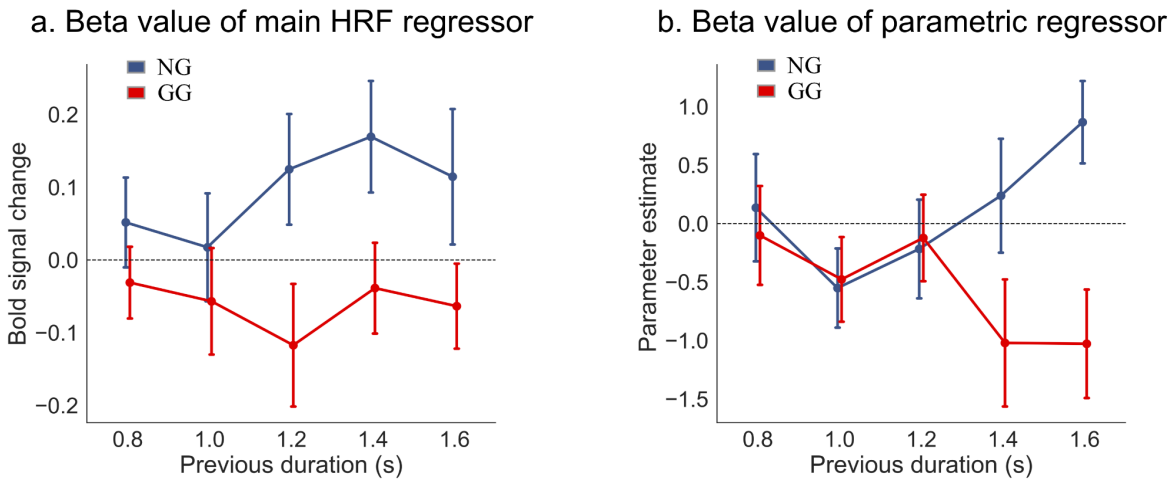

Figure 5 (**a**) BOLD signal change estimated from the hippocampus, plotted as a function of previous duration, separated for the previous task (NG: No-Go, GG: Go). (**b**) Mean beta value of the parametric regressor extracted from the bilateral hippocampus (MNI coordinates: -36, -37, -7, including 139 voxels; MNI coordinates: 39, -31, -7, including 305 voxels) plotted as a function of previous durations, separated for the previous task (NG: No-Go, GG: Go).

Note that in the whole brain analysis, we observed a large significant activated cluster (consisting of 8003 voxels) in the contrast NG > GG analysis (see Table 1), which included 0.7% (56 voxels) of this cluster that belonged to the hippocampus. To more closely examine the neural activation patterns in the bilateral hippocampus in the cluster we obtained in our ROI analysis (MNI coordinates: -36, -37, -7, including 139 voxels; MNI coordinates: 39, -31, -7, including 305 voxels), we applied a separate GLM on BOLD signals to model the previous tasks (GG vs. NG) with each of the five previous durations (0.8, 1.0, 1.2, 1.4, and 1.6 s) for individual subject, and extracted the β values from the main and parametric regressors. The β values of the main HRF regressors are shown in Figure 5a. Across all previous durations, the activations were generally higher for NG than for GG trials. Further linear mixed model on the β values with the fixed factors of Prior Duration and Prior Task and participants as a random factor revealed a significant difference between prior tasks (b = 0.16, 95% CI [0.08, 0.233], $p < .001$), but not among prior durations and the interaction between Prior

Task and Prior Duration (all *p*s > .239). On average, trials with preceding passive viewing, compared to trials with preceding active reproduction, had 16% more activations in the hippocampus.

Figure 5b shows that the parametric value decreases with an increase in the previous duration for the GG condition, but increases for the NG condition. A linear mixed model on the parametric values with fixed factors of Prior Duration and Prior Task revealed a significant main effect of Prior Task (b = 0.64, 95% *CI* [0.12, 1.17], p = .016), and a significant interaction between Prior Task and Prior Duration (b = 2.32, 95% *CI* [0.48, 4.17], p = .014). The interaction was due to opposite linear trends observed between the parametric values and the previous duration for the NG and GG conditions: a positive trend for the NG (b = 1.13, 95% CI [-0.18, 2.43], p = .091), but a negative trend for the GG (b = -1.20, 95% CI [-2.50, 0.11], p = .072). Although the individual trends (the slopes of 1.13 vs. -1.20) were marginal significant from zero, the difference between the two (b = 2.32) was significant, particularly for the previous long durations (Figure 5b). Interestingly, for the GG condition, the negative trend of the parametric value with the previous long duration was *opposite* to the significant positive trend of the sequential dependence effect (Figure 2b). This implies that decreased brain activity in the hippocampus was associated with a high normalized error, possibly due to the recycling of prior information in working memory, which results in strong sequential dependence (Sheehan and Serences, 2022; Whitney et al., 2022).

Discussion

This study investigated neural mechanisms that underlie sequential dependence in time perception. We conducted a duration reproduction task with a post-cue to manipulate between active reproduction and passive viewing of durations, aiming to determine where the sequential dependence originates. We found a strong central tendency effect in duration reproduction, regardless of the preceding task. However, the normalized reproduced error, measured relative to the mean reproduction of individual durations, depended on the preceding task and duration, showing a positive sequential dependence effect only for trials with consecutive reproduction (GG), but not for trials preceded by passive viewing (NG).

Our study seeks to expand upon previous research, which has primarily focused on sequential dependence in non-temporal domains (e.g., Holland and Lockhead, 1968; Fischer and Whitney, 2014). Previous studies have shown that sequential dependence requires active retrieval of a memory trace (Bae and Luck, 2020; Fornaciai and Park, 2020b; Ranieri et al., 2022). For instance, a study on motion direction judgment (Bae & Luck, 2020) revealed that sequential dependence was only present when the preceding task was identical, as opposed to being different, such as judging the color of the motion stimuli. Other studies have also concurred with the idea that sequential dependence is driven by the reactivation of memory trace during conducting the same task, rather than simply the memory trace itself (Fornaciai and Park, 2020b; Ranieri et al., 2022). Our study extends this research by demonstrating that in the temporal domain, simply encoding the previous stimulus was not enough to produce a sequential effect. Instead, sequential dependence required the involvement of decisional templates that link sensory representation and responses. Thus, the sequential dependence in time perception likely stems from high-level, post-perceptual decisional processes (Fritsche et al., 2017; Kiyonaga et al., 2017; Pascucci et al., 2019; Bae and Luck, 2020; Ceylan et al., 2021).

At the neuronal level, BOLD signals at the duration encoding phase were enhanced for NG trials relative to GG trials in a cognitive control and response preparation network (Ridderinkhof et al., 2004; Chris Dijkerman and de Haan, 2007; Fitzgerald et al., 2010) comprising the right posterior-medial frontal, the left postcentral gyrus, and the left Precueus. Additionally, the right thalamus, a critical component of cortico-thalamic-basal ganglia timing circuits (Mole et al., 2018; Yin et al., 2022), was activated. These differential activations were likely attributed to the passive viewing vs. active reproduction in the previous trial. Following a passive viewing with no response demands, the response preparation network and the cortico-thalamic-basal ganglia timing circuits were more effectively primed for the next upcoming trial. In a simulation (Appendix), we showed that early activation of motor regions for NG trials compared to GG trials could explain the motor cortex activities we observed. In contrast, the right inferior frontal gyrus (RIFG), a crucial region for response inhibition and detection of important cues (Aron et al., 2007; Hampshire et al., 2010; Hartwigsen et al., 2019), was more active for GG trials than for NG trials. This is because following

an active reproduction trial, the next trial could be either Go or No-go trials, which can only be resolved when the post cue appears.

The contrast between the prior long and short durations revealed greater activation in the right caudate nucleus for the prior long duration. The caudate nucleus, a key part of the dorsal striatum, plays a critical role in the striato-thalamo-cortical network (Rao et al., 2001; Coull and Nobre, 2008; Teki and Griffiths, 2016). Serving as a 'core timer' of the timing system (Meck et al., 2008), the caudate nucleus holds temporal 'memories' in its GABAergic medium spiny neurons (MSNs) via dopamine-facilitated long-term potentiation and short-term plasticity mechanisms (Allman and Meck, 2012; Kononowicz, 2015). Adjustments to corticostriatal synaptic weights by MSNs in the dorsal striatum could tune them to specific time intervals encoded by coincident oscillatory patterns, increasing the likelihood of them firing upon similar intervals in the future (Kononowicz et al., 2016; Yin et al., 2022). The observed sequential dependence in the present study likely reflects these residual temporal 'memories' left in the MSNs of the caudate nucleus from the previous trial.

Using parametric modulation analysis on the brain activity, which could reflect how the sequential bias covaries with BOLD activations, we found that the left middle frontal gyrus showed greater sensitivity to sequential bias when the prior duration was long compared to short. The left middle frontal gyrus is widely recognized to contribute to working memory encoding (Nee et al., 2013; Dandolo and Schwabe, 2019) through the fronto-striatal pathway (Darki and Klingberg, 2015; Teki and Griffiths, 2016). This was evidenced by previous research showing that activity in the caudate nucleus and the frontal cortex systematically increased with an increasing number of intervals in the sequence (Rao et al., 2001; Coull and Nobre, 2008; Teki and Griffiths, 2016), indicating a close relationship between perception and memory for the time in fronto-striatal pathways (Matell et al., 2005). Our findings thus suggest that the strong modulation of sequential bias in the left frontal gyrus may be due to the high involvement of working memory encoding and fronto-strialatal timing circuits in processing prior long durations.

Furthermore, the ROI analysis revealed that the sequential bias was sensitive to brain activities in the hippocampus. Together with the preparation network that includes the precuneus, the hippocampus was more active for NG trials than for GG trials. Previous research has indicated that

the precuneus receives connections from the hippocampal system and is involved in working memory (Hebscher et al., 2018; Ren et al., 2018). The increased activation of the response preparation network and hippocampus during NG trials may reflect the process that the previously encoded duration (in the No-go trial) was task-irrelevant, so it needs to be overwritten with the task-relevant duration in the following Go trial. It may indicate a more efficient encoding of the duration and retention in working memory in the NG trials, preventing inter-trial memory interference and reducing any bias from the past. This could explain why the behavioral results showed less sequential bias in NG trials than in GG trials. In contrast, the attenuation in the hippocampus found in the GG condition might be linked to recycling the prior trial information in working memory, which causes sequential dependence (Sheehan and Serences, 2022; Whitney et al., 2022). This reduction in neural signal associated with the bias may reflect an optimal allocation of cognition resources to process successive stimuli (Hsieh et al., 2014; Chanales et al., 2017). It is worth noting that we observed a negative correlation between BOLD signals and the strength of sequential biases across participants, but only for GG trials. This correlation was absent for NG trials (Figure 4c). Given the lower activation of the hippocampus during GG trials, the sequential bias was more likely to be influenced by fluctuations in BOLD signals from the hippocampus, with a higher sequential bias for a lower BOLD signal.

The hippocampus and the dorsal striatum collaborate to process temporal expectations based on past experience (van de Ven et al., 2020). Our study indicates that when the hippocampus is actively engaged, sensory encoding of the current duration information held in working memory is effectively protected, resulting in less sequential bias. A recent study using TMS to disrupt the left dorsal premotor cortex, a region critical to short-term memory, during intertrial intervals showed a significant reduction of serial dependence for motion speed judgments (de Azevedo Neto and Bartels, 2021), indicating that memory mixing during maintenance is the primary source of sequential dependence. Moreover, A recent fMRI study found a sequential assimilation effect in behavior during a delayed orientation discrimination task, but repulsive BOLD signals in the early sensory cortex (Sheehan and Serences, 2022), suggesting sequential assimilation arises in either memory or decision-making circuits rather than early sensory areas. Similarly, here we observed a negative modulation in the hippocampus by prior reproduction on current encoding, as well as a negative

correlation between hippocampus BOLD signals and sequential bias in behavior, further confirming the crucial role of memory in the inter-trial sequential bias.

Importantly, our study extends current research of sequential effect into the temporal domain, indicating that sequential dependence in temporal perception requires the involvement of decision templates that link sensory representation and responses. In addition, we used fMRI to develop a parametric modulation model that links measured neural activities to behavioral bias, and the physiological results provide neural signatures, such as the hippocampus linked to the bias tuning properties of serial dependence in time perception. The primary exploration is an important step for linking behavior and physiology in sequential dependence research of non-spatial domains. While our findings highlight the critical role of memory networks in sequential dependence, this does not preclude involvement of the sensory cortex. Previous literature has shown that serial dependence emerges early in the perceptual processing, and occurred in the visual cortex when exposed to visual stimuli (St. John-Saaltink et al., 2016; Fornaciai and Park, 2020b), as well as the premotor cortex during visuomotor integration (de Azevedo Neto and Bartels, 2021). Convergent evidence shows that sequential dependence could emerge at different stages. However, our study using the post-cue paradigm suggested that the sequential effect in the time domain relies heavily on late decision stages that engage working memory, partly because duration perception requires less perceptual stability. Future work could go further into detail and investigate possible connectivity between cortico-thalamic-basal ganglia timing circuits and memory related networks underlying sequential dependence in time perception. Furthermore, prior research has shown that the strength of serial dependence increases with longer memory retention (Bliss et al., 2017), further study is necessary to explore how working-memory retention affects the neural correlates of serial dependence directly and which hippocampal subfields, such as the CA1, CA2, subiculum, etc., interact with timing networks and play a key role in such sequential bias (Robert et al., 2021).

In summary, our study revealed that sequential dependence in duration reproduction is contingent on the task of the preceding trial. Memory and striato-thalamo-cortical networks were actively engaged during trials preceded by passive viewing, resulting in the absence of sequential bias. In contrast, the hippocampus was less active during trials with consecutive reproduction, leading to

prominent sequential biases, which negatively correlated with hippocampal activation across individuals. These findings highlight that sequential dependence in temporal perception requires the involvement of the post-perceptual stage that links sensory representations and responses, and the hippocampus plays a key role in this process.

Reference

Abraham A, Pedregosa F, Eickenberg M, Gervais P, Mueller A, Kossaifi J, Gramfort A, Thirion B, Varoquaux G (2014) Machine learning for neuroimaging with scikit-learn. Front Neuroinform 8:14.

Allman MJ, Meck WH (2012) Pathophysiological distortions in time perception and timed performance. Brain 135:656–677 Available at: http://dx.doi.org/10.1093/brain/awr210.

Aron AR, Behrens TE, Smith S, Frank MJ, Poldrack RA (2007) Triangulating a cognitive control network using diffusion-weighted magnetic resonance imaging (MRI) and functional MRI. J Neurosci 27:3743–3752.

Ashburner J, Barnes G, Chen C, Daunizeau J, Flandin G, Friston K, Kiebel S, Kilner J, Litvak V, Moran R, Others (2014) SPM12 manual. Wellcome Trust Centre for Neuroimaging, London, UK:2464.

Bae G-Y, Luck SJ (2019) Reactivation of Previous Experiences in a Working Memory Task. Psychol Sci 30:587–595.

Bae G-Y, Luck SJ (2020) Serial dependence in vision: Merely encoding the previous-trial target is not enough. Psychon Bull Rev 27:293–300.

Barbosa J, Compte A (2020) Build-up of serial dependence in color working memory. Sci Rep 10:10959.

Bliss DP, Sun JJ, D'Esposito M (2017) Serial dependence is absent at the time of perception but increases in visual working memory. Sci Rep 7:1–13.

Burr DC, Banks MS, Morrone MC (2009) Auditory dominance over vision in the perception of interval duration. Exp Brain Res 198:49–57.

Ceylan G, Herzog MH, Pascucci D (2021) Serial dependence does not originate from low-level visual processing. Cognition 212:104709.

Chanales AJH, Oza A, Favila SE, Kuhl BA (2017) Overlap among Spatial Memories Triggers Repulsion of Hippocampal Representations. Curr Biol 27:2307–2317.e5.

Chris Dijkerman H, de Haan EHF (2007) Somatosensory processes subserving perception and action. Behav Brain Sci 30:189–201.

Cicchini GM, Anobile G, Burr DC (2014) Compressive mapping of number to space reflects dynamic encoding mechanisms, not static logarithmic transform. Proc Natl Acad Sci U S A 111:7867–7872.

Cicchini GM, Arrighi R, Cecchetti L, Giusti M, Burr DC (2012) Optimal encoding of interval timing in expert percussionists. J Neurosci 32:1056–1060.

Cicchini GM, Mikellidou K, Burr D (2017) Serial dependencies act directly on perception. J Vis 17:6.

Cicchini GM, Mikellidou K, Burr DC (2018) The functional role of serial dependence. Proc Biol Sci 285 Available at: http://dx.doi.org/10.1098/rspb.2018.1722.

Coull J, Nobre A (2008) Dissociating explicit timing from temporal expectation with fMRI. Curr Opin Neurobiol 18:137–144.

Czoschke S, Fischer C, Beitner J, Kaiser J, Bledowski C (2019) Two types of serial dependence in visual working memory. Br J Psychol 110:256–267.

Dandolo LC, Schwabe L (2019) Time-dependent motor memory representations in prefrontal cortex. Neuroimage 197:143–155.

Darki F, Klingberg T (2015) The role of fronto-parietal and fronto-striatal networks in the development of working memory: a longitudinal study. Cereb Cortex 25:1587–1595.

de Azevedo Neto RM, Bartels A (2021) Disrupting Short-Term Memory Maintenance in Premotor Cortex Affects Serial Dependence in Visuomotor Integration. J Neurosci 41:9392–9402.

Debener S, Ullsperger M, Siegel M, Fiehler K, von Cramon DY, Engel AK (2005) Trial-by-trial coupling of concurrent electroencephalogram and functional magnetic resonance imaging identifies the dynamics of performance monitoring. J Neurosci 25:11730–11737.

Dyjas O, Bausenhart KM, Ulrich R (2012) Trial-by-trial updating of an internal reference in discrimination tasks: evidence from effects of stimulus order and trial sequence. Atten Percept Psychophys 74:1819–1841.

Erdfelder E, Faul F, Buchner A (1996) GPOWER: A general power analysis program. Behav Res Methods Instrum Comput 28:1–11.

Fischer J, Whitney D (2014) Serial dependence in visual perception. Nat Neurosci 17:738–743.

Fitzgerald KD, Perkins SC, Angstadt M, Johnson T, Stern ER, Welsh RC, Taylor SF (2010) The development of performance-monitoring function in the posterior medial frontal cortex. Neuroimage 49:3463–3473.

Fornaciai M, Park J (2020a) Attractive serial dependence between memorized stimuli. Cognition 200:104250.

Fornaciai M, Park J (2020b) Neural Dynamics of Serial Dependence in Numerosity Perception. J Cogn Neurosci 32:141–154.

Fritsche M, Mostert P, de Lange FP (2017) Opposite Effects of Recent History on Perception and Decision. Curr Biol 27:590–595.

Glasauer S, Shi Z (2022) Individual beliefs about temporal continuity explain variation of perceptual biases. Sci Rep 12:10746.

Hampshire A, Chamberlain SR, Monti MM, Duncan J, Owen AM (2010) The role of the right inferior frontal gyrus: inhibition and attentional control. Neuroimage 50:1313–1319.

Hari R, Forss N, Avikainen S, Kirveskari E, Salenius S, Rizzolatti G (1998) Activation of human primary motor cortex during action observation: a neuromagnetic study. Proc Natl Acad Sci U S

A 95:15061–15065.

Hartwigsen G, Neef NE, Camilleri JA, Margulies DS, Eickhoff SB (2019) Functional Segregation of the Right Inferior Frontal Gyrus: Evidence From Coactivation-Based Parcellation. Cereb Cortex 29:1532–1546.

Hebscher M, Levine B, Gilboa A (2018) The precuneus and hippocampus contribute to individual differences in the unfolding of spatial representations during episodic autobiographical memory. Neuropsychologia 110:123–133.

Holland MK, Lockhead GR (1968) Sequential effects in absolute judgments of loudness. Percept Psychophys 3:409–414.

Hsieh L-T, Gruber MJ, Jenkins LJ, Ranganath C (2014) Hippocampal Activity Patterns Carry Information about Objects in Temporal Context. Neuron 81:1165–1178.

Jazayeri M, Shadlen MN (2010) Temporal context calibrates interval timing. Nat Neurosci 13:1020–1026.

Kiyonaga A, Scimeca JM, Bliss DP, Whitney D (2017) Serial Dependence across Perception, Attention, and Memory. Trends Cogn Sci 21:493–497.

Kononowicz TW (2015) Dopamine-dependent oscillations in frontal cortex index “start-gun” signal in interval timing. Front Hum Neurosci 9 Available at: https://www.frontiersin.org/articles/10.3389/fnhum.2015.00331.

Kononowicz TW, van Rijn H, Meck WH (2016) Timing and time perception: a critical review of neural timing signatures before, during, and after the To-Be-Timed Interval. Stevens Handbook of Experimental Psychology and Cognitive Neuroscience (4th ed).

Liberman A, Zhang K, Whitney D (2016) Serial dependence promotes object stability during occlusion. J Vis 16:16.

Lund TE, Nørgaard MD, Rostrup E, Rowe JB, Paulson OB (2005) Motion or activity: their role in intra- and inter-subject variation in fMRI. Neuroimage 26:960–964.

Matell MS, Meck WH, Lustig C (2005) Not “just” a coincidence: Frontal‐striatal interactions in working memory and interval timing. Memory 13:441–448.

Meck WH, Penney TB, Pouthas V (2008) Cortico-striatal representation of time in animals and humans. Curr Opin Neurobiol 18:145–152.

Merchant H, Harrington DL, Meck WH (2013) Neural Basis of the Perception and Estimation of Time. Annu Rev Neurosci Available at: http://dx.doi.org/10.1146/annurev-neuro-062012-170349.

Mole J, Winegardner J, Malley D, Fish J (2018) Time perception impairment following thalamic stroke: A case study. Neuropsychol Rehabil 28:208–222.

Mumford (2015) Orthogonalization of Regressors in fMRI Models. PLOS ONE Available at: https://journals.plos.org/plosone/article?id=10.1371/journal.pone.0126255.

Nakajima Y, ten Hoopen G, Hilkhuysen G, Sasaki T (1992) Time-shrinking: a discontinuity in the perception of auditory temporal patterns. Percept Psychophys 51:504–507.

Nee DE, Brown JW, Askren MK, Berman MG, Demiralp E, Krawitz A, Jonides J (2013) A meta-analysis of executive components of working memory. Cereb Cortex 23:264–282.

Pascucci D, Mancuso G, Santandrea E, Della Libera C, Plomp G, Chelazzi L (2019) Laws of concatenated perception: Vision goes for novelty, decisions for perseverance. PLoS Biol 17:e3000144.

Penny WD, Friston KJ, Ashburner JT, Kiebel SJ, Nichols TE (2011) Statistical Parametric Mapping: The Analysis of Functional Brain Images. Elsevier.

Ranieri G, Benedetto A, Ho HT, Burr DC, Morrone MC (2022) Evidence of Serial Dependence from Decoding of Visual Evoked Potentials. J Neurosci 42:8817–8825.

Rao SM, Mayer AR, Harrington DL (2001) The evolution of brain activation during temporal processing. Nat Neurosci 4:317–323.

Ren Y, Nguyen VT, Sonkusare S, Lv J, Pang T, Guo L, Eickhoff SB, Breakspear M, Guo CC (2018) Effective connectivity of the anterior hippocampus predicts recollection confidence during natural memory retrieval. Nat Commun 9:4875.

Ridderinkhof KR, Ullsperger M, Crone EA, Nieuwenhuis S (2004) The role of the medial frontal cortex in cognitive control. Science 306:443–447.

Roach NW, McGraw PV, Whitaker DJ, Heron J (2017) Generalization of prior information for rapid Bayesian time estimation. Proceedings of the National Academy of Sciences 114:412–417.

Robert V, Therreau L, Chevaleyre V, Lepicard E, Viollet C, Cognet J, Huang AJ, Boehringer R, Polygalov D, McHugh TJ, Piskorowski RA (2021) Local circuit allowing hypothalamic control of hippocampal area CA2 activity and consequences for CA1. Elife 10 Available at: http://dx.doi.org/10.7554/eLife.63352.

Robinson JL, Laird AR, Glahn DC, Blangero J, Sanghera MK, Pessoa L, Fox PM, Uecker A, Friehs G, Young KA, Griffin JL, Lovallo WR, Fox PT (2012) The functional connectivity of the human caudate: an application of meta-analytic connectivity modeling with behavioral filtering. Neuroimage 60:117–129.

Sheehan TC, Serences JT (2022) Attractive serial dependence overcomes repulsive neuronal adaptation. PLoS Biol 20:e3001711.

Shi Z, Church RM, Meck WH (2013a) Bayesian optimization of time perception. Trends Cogn Sci 17:556–564.

Shi Z, Ganzenmüller S, Müller HJ (2013b) Reducing bias in auditory duration reproduction by integrating the reproduced signal. PLoS One 8:e62065.

Shi Z, Theisinger LA, Allenmark F, Pistorius RL, Müller HJ, Falter-Wagner CM (2022) Predictive coding in ASD: inflexible weighting of prediction errors when switching from stable to volatile environments. bioRxiv:2022.01.21.477218 Available at: https://www.biorxiv.org/content/biorxiv/early/2022/01/25/2022.01.21.477218 [Accessed February 10, 2022].

Singmann H, Kellen D (2019) An introduction to mixed models for experimental psychology. In: New Methods in Cognitive Psychology, pp 4–31. Routledge.

St. John-Saaltink E, Kok P, Lau HC, de Lange FP (2016) Serial Dependence in Perceptual Decisions Is Reflected in Activity Patterns in Primary Visual Cortex. J Neurosci 36:6186–6192.

Teki S, Griffiths TD (2016) Brain Bases of Working Memory for Time Intervals in Rhythmic Sequences. Front Neurosci 10:239.

Treisman M, Williams TC (1984) A theory of criterion setting with an application to sequential dependencies. Psychol Rev 91:68–111.

van de Ven V, Lee C, Lifanov J, Kochs S, Jansma H, De Weerd P (2020) Hippocampal-striatal functional connectivity supports processing of temporal expectations from associative memory. Hippocampus 30:926–937.

White NM (2009) Some highlights of research on the effects of caudate nucleus lesions over the past 200 years. Behav Brain Res 199:3–23.

Whitney D, Manassi M, Murai Y (2022) Searching for serial dependencies in the brain. PLoS Biol 20:e3001788.

Wittmann M (2009) The inner experience of time. Philos Trans R Soc Lond B Biol Sci 364:1955–1967.

Yin B, Shi Z, Wang Y, Meck WH (2022) Oscillation/coincidence-detection models of reward-related timing in corticostriatal circuits. Timing Time Percept:1–43.

Zang X, Zhu X, Allenmark F, Wu J, Müller HJ, Glasauer S, Shi Z (2022) Duration reproduction under memory pressure: Modeling the roles of visual memory load in duration encoding and reproduction. bioRxiv:2022.02.10.479853 Available at: https://www.biorxiv.org/content/10.1101/2022.02.10.479853v1 [Accessed March 4, 2022].